

NRL Report 6129

# Theoretical Design of Primary and Secondary Cells

## Part IV - Further Studies of the Battery Discharge Equation

C. M. SHEPHERD

*Electrochemistry Branch  
Chemistry Division*

November 16, 1964



**U.S. NAVAL RESEARCH LABORATORY**  
Washington, D.C.

PREVIOUS REPORTS IN THIS SERIES

"Part I - Effect of Polarization and Internal Resistance on Current Density Distribution," C.M. Shepherd, NRL Report 5211, Dec. 29, 1958

"Part II - Effect of Polarization and Internal Resistance on Cell Characteristics and Cell Design," C.M. Shepherd, NRL Report 5212, Dec. 30, 1958

"Part III - Battery Discharge Equation," C.M. Shepherd, NRL Report 5908, May 2, 1963

## CONTENTS

Abstract	ii
Problem Status	ii
Authorization	ii
INTRODUCTION	1
MATHEMATICAL ANALYSIS	1
Basic Assumptions	1
Derivation of Equation	2
FITTING THE EQUATION NUMERICALLY TO EXPERIMENTAL DATA	4
DISCUSSION OF THE EQUATION AND ITS APPLICATION	8
CONCLUSIONS	13
APPENDIX - Actual Discharge Data Used for Calculation of Battery Discharge Equation	14
REFERENCES	24

## ABSTRACT

An equation has been derived describing a complete battery discharge for the case where the current density is constant. The battery potential during discharge is given as a function of time, current density, polarization, internal resistance, and other factors. This equation has a number of practical applications. It can be used to describe battery charges, discharges, capacities, power evolution, and to predict capacities and locate errors in experimental data. A simplified numerical system has been developed for determining the equation constants from the experimental data.

## PROBLEM STATUS

This is an interim report; work is continuing.

## AUTHORIZATION

NRL Problem CO5-14  
Projects SF 013-06-03-4366 and  
RR 001-01-43-4755

Manuscript submitted June 4, 1964.

# THEORETICAL DESIGN OF PRIMARY AND SECONDARY CELLS

## Part IV - Further Studies of the Battery Discharge Equation

REF ID: A70100

### INTRODUCTION

This paper is one of a series whose ultimate goal is to determine procedures for designing batteries having optimum properties such as minimum weight or minimum volume. In particular, the derivation and application of an equation describing battery discharge given previously\* will be more fully discussed. This equation gives the cell potential during discharge as a function of discharge time, current density, and certain other factors and it can also be used to describe battery charge curves, capacities, power evolution, and to predict capacities on the basis of limited data.\* This equation can be used to pinpoint variations in the discharge data due to experimental error, uncontrolled variables, etc.; thus minimizing the amount of experimental data needed.

A complete set of discharge curves can be described by a single equation therefore making it possible to present in less space a more detailed description of cell characteristics than has been customary in battery papers.

### MATHEMATICAL ANALYSIS

#### Basic Assumptions

The mathematical analysis given here is based on the assumption that the following conditions are applicable:

1. The anode and/or cathode have porous active materials.
2. The electrolyte resistance is constant throughout discharge.
3. The battery is discharged at a constant current.
4. The polarization is a linear function of the active material current density.

When ionic discharge is the slow or rate determining process, the relationship between steady-state current density and activation overpotential at an electrode is usually written as

$$i = i_0 e^{a\eta ZF/RT} - i_0 e^{-(1-a)\eta ZF/RT}, \quad (1)$$

where  $i$  is the apparent current density in amperes per  $\text{cm}^2$ ,  $i_0$  is the apparent exchange current density in amperes per  $\text{cm}^2$ ,  $\alpha$  is the transfer coefficient ( $0 \leq \alpha \leq 1$ ),  $Z$  is the number of electrons transferred in the rate-determining step,  $F$  is the faraday,  $R$  is the gas constant, and  $T$  is the temperature in  $^\circ\text{K}$ . The steady state activation overpotential  $\eta$  is positive for the deposition of cations.

\*C.M. Shepherd, "Theoretical Design of Primary and Secondary Cells, Part 3 - Battery Discharge Equation," NRL Report 5908, May 2, 1963.

When the exponential terms are expanded as a series, powers greater than one can be neglected if  $\eta$  is sufficiently small and Eq. (1) becomes

$$i = i_o \left( \frac{\eta ZF}{RT} \right) \quad (2)$$

or

$$\eta = \left( \frac{RT}{ZF i_o} \right) i ; \quad (3)$$

thus establishing a linear relationship between  $\eta$  and  $i$  which is fairly accurate up to the values of  $\eta$  equal to approximately 0.03 volt. If Eq. (1) is applicable to a battery, the variation of  $\eta$  with change in  $i$  can be fitted by a straight line within approximately 0.02 to 0.04 volt up to values of  $\eta$  equal to about 0.2 to 0.4 volt. A potential drop of this magnitude would cover the major portion of the polarization that occurs during most battery discharges.

#### Derivation of Equation

In Fig. 1, two solid curves are shown which represent typical battery discharges. The potential in volts is plotted as a function of  $i t$ , the quantity of electricity that has been obtained from the battery at time  $t$ . It is assumed in the derivation that follows that the polarization is linear to the right of point b. If all factors except polarization are ignored, then  $E_c$ , the cathode potential during discharge, is defined as

$$E_c = E_{sc} - K_c i_{am} , \quad (4)$$

where  $E_{sc}$  is a constant potential,  $K_c$  is the cathode coefficient of polarization per unit current density, and  $i_{am}$  is the active material current density.

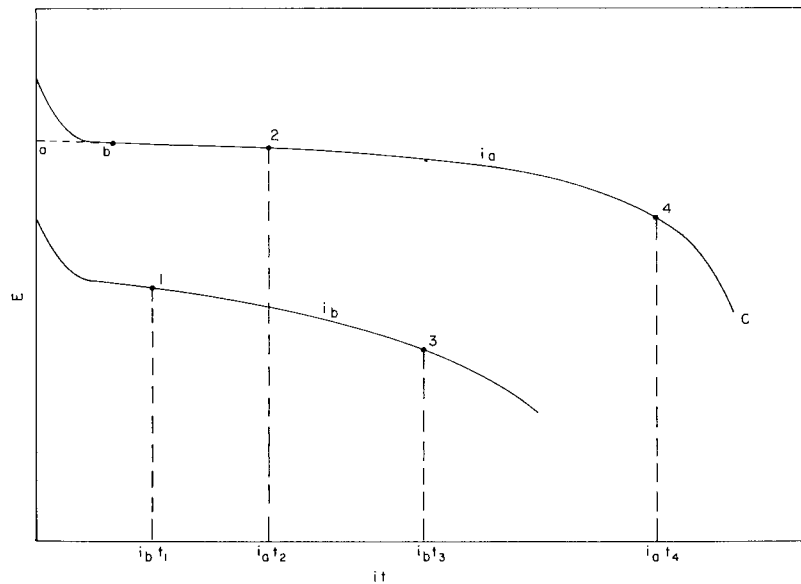


Fig. 1 - Typical discharge curves used in equation fitting

The successful use of Eq. (4) as a fundamental equation in the derivation that follows does not necessarily imply that the theoretical factors associated with Eq. (1) apply to most battery discharges even though both equations are linear.

The active material current density  $i_{am}$  is defined as being inversely proportional to the amount of unused active material and is also equal to  $i$  at the beginning of the discharge. Thus if two-thirds of the active material is used up at some point in the discharge, one-third of it is left and the active material current density is three times what it was at the beginning of the discharge or  $3i$ . Consequently

$$i_{am} = \left( \frac{Q_c}{Q_c - it} \right) i, \quad (5)$$

where  $t$  is the time at any point during the discharge and  $Q_c$  is the amount of available cathode active material expressed in units such as coulombs or ampere hours per unit area.  $Q_c$  is not necessarily the total amount of active material, but is simply the amount that is available for discharge purposes.

When Eq. (5) is substituted in Eq. (4)

$$E_c = E_{sc} - K_c \left( \frac{Q_c}{Q_c - it} \right) i. \quad (6)$$

Similarly,

$$E_a = E_{sa} - K_a \left( \frac{Q_a}{Q_a - it} \right) i, \quad (7)$$

where the subscripts  $a$  and  $c$  denote the anode and cathode values for the constants respectively. A sign convention is used here which makes the value of the potential terms positive.

If  $Q_a$  is approximately equal to  $Q_c$ , as it generally is in a well designed battery, Eqs. (6) and (7) can be summed to give

$$E = E_s - K \left( \frac{Q}{Q - it} \right) i, \quad (8)$$

where  $E = E_a + E_c$  is the potential of the battery (neglecting the internal resistance) at any time  $t$  during the discharge;  $E_s = E_{sa} + E_{sc}$  is a constant potential;  $K = K_a + K_c$  is the polarization coefficient in ohm  $\text{cm}^2$ , and  $Q = Q_a = Q_c$  is the available amount of active material in coulombs or similar units per unit area.

If  $Q_a$  is appreciably larger than  $Q_c$ , then the numerical increase in the value of the last term in Eq. (7) will be small compared to the numerical increase in the value of the last term of Eq. (6) as  $it$  approaches  $Q_c$  in value. Consequently the second term of Eq. (7) can be considered to be approximately constant and the sum of Eqs. (6) and (7) will still have approximately the form shown in Eq. (8). Under these conditions the approximate values of  $K$ ,  $Q$ , and  $E_s$  will be  $K = K_c$ ,  $Q = Q_c$ , and  $E_s = E_{sa} + E_{sc} - K_a i$ .

When the potential drop due to internal resistance is considered, Eq. (8) becomes

$$E = E_s - K \left( \frac{Q}{Q - it} \right) i - Li, \quad (9)$$

where  $L$ , the internal resistance per unit area, is measured in ohm  $\text{cm}^2$  or other suitable units.

When Eq. (9) is evaluated mathematically, a set of curves is obtained, one of which is plotted in Fig. 1 as a dotted line from  $a$  to  $b$  and a solid line from  $b$  to  $c$ . The initial drop in potential at the beginning of a battery discharge is not included in Eq. (9). Consequently another term must be added to correct for the difference between the dotted line potential calculated from Eq. (9) and the solid line that represents the actual discharge potential. It has been found that the expression  $Ae^{-Bt/Q}$ , where  $A$  and  $B$  are empirical constants, gives an excellent estimate of the initial potential drop in virtually every case. When this term is added to Eq. (9), the final equation

$$E = E_s - K \left( \frac{Q}{Q - it} \right) i - Li + Ae^{-Bt/Q} \quad (10)$$

is obtained. In a number of cases the initial drop in potential is too rapid to affect the observed experimental data appreciably and consequently the value of  $Ae^{-Bt/Q}$  is negligible.

That portion of the discharge curve that lies to the right of point  $b$  in Fig. 1 could be predicted from Eq. (10) if the numerical values of  $E_s$ ,  $K$ ,  $Q$ , and  $L$  were known, providing the basic assumptions were true. However, the labor involved in determining these values would be so large that it probably would be easier, and certainly more accurate, to determine discharge curves experimentally. However, Eq. (10) can be fitted numerically to experimental discharge data, thus determining empirical values of  $E_s$ ,  $K$ ,  $Q$ ,  $L$ ,  $A$ , and  $B$ . Such a numerical equation gives an accurate description of the battery discharge and can be used to describe energy evolution, cell capacity, and in predicting cell capacities. Despite its successful applications, it must be considered to be an empirical equation since the numerical values of  $K$ ,  $Q$ , and  $L$  that are determined in this manner will vary considerably at times from their true values as defined in the basic assumptions.

#### FITTING THE EQUATION NUMERICALLY TO EXPERIMENTAL DATA

There are a number of methods that can be used to determine the numerical values of  $E_s$ ,  $K$ ,  $Q$ ,  $L$ ,  $A$ , and  $B$  in Eq. (10) from experimental discharge data, most of which are unsuitable. The least squares solution is particularly involved and time-consuming. The following approach is easily applied, rapid, reasonably accurate, and is used in fitting Eq. (10) to discharges made at a number of current densities.

In Fig. 1, four points, labeled 1, 2, 3, and 4, have been selected on two discharge curves which were obtained at the moderately low current density,  $i_a$ , and the moderately high current density,  $i_b$ . The values of  $E$  and  $it$  at points 1, 2, 3, and 4, are  $E_1$ ,  $E_2$ ,  $E_3$ , and  $E_4$  and  $i_b t_1$ ,  $i_a t_2$ ,  $i_b t_3$ , and  $i_a t_4$ , respectively. These four points are chosen to the right of the initial potential drop. Thus the value of  $Ae^{-Bt/Q}$  is negligible and the potential at point 2 is found from Eq. (10) to be approximately

$$E_2 = E_s - K \left( \frac{Q}{Q - i_a t_2} \right) i_a - Li_a \quad (11)$$

Similarly,

$$E_4 = E_s - K \left( \frac{Q}{Q - i_a t_4} \right) i_a - Li_a \quad (12)$$

Subtracting Eq. (12) from Eq. (11) gives

$$E_2 - E_4 = Ki_a \left[ \frac{Q(i_a t_4 - i_a t_2)}{(Q - i_a t_4)(Q - i_a t_2)} \right] \quad (13)$$

The equation for  $E_1 - E_3$  is obtained in a similar manner and is divided into Eq. (13) to give

$$\frac{E_2 - E_4}{E_1 - E_3} = \frac{i_a}{i_b} \left( \frac{i_a t_4 - i_a t_2}{i_b t_3 - i_b t_1} \right) \frac{(Q - i_b t_3)(Q - i_b t_1)}{(Q - i_a t_4)(Q - i_a t_2)} \quad (14)$$

When numerical values of the  $E$ 's,  $i$ 's, and  $it$ 's are taken from the discharge data in Fig. 2 and substituted in Eq. (14), a quadratic equation in  $Q$  is obtained which is solved to give a numerical value of  $Q$ . This value of  $Q$  is substituted in Eq. (13) and solved to obtain a numerical value of  $K$ . When these values of  $Q$  and  $K$  are substituted in Eq. (11) and a similar equation for  $E_1$ , two simultaneous equations are obtained which may be solved to give numerical values for  $E_s$  and  $L$ . When these values of  $E_s$ ,  $L$ ,  $K$ , and  $Q$  are substituted in Eq. (10),  $E$  is obtained as a specific function of  $it$ . The exponential term  $Ae^{-B it/Q}$  is determined by difference. The calculation of  $Q$  by use of Eq. (14) can generally be simplified by choosing point 2 in a manner such that  $i_a t_2$  equals either  $i_b t_3$  or  $i_b t_1$ .

The two discharge curves,  $i_a$  and  $i_b$ , that are chosen as a basis for these calculations should be representative of the complete set of discharge curves and should show no obvious visual discrepancies that would indicate variations not present in the other curves. They are selected in the following manner. If  $it$  is held constant, Eq. (10) shows that the potential  $E$  to the right of point  $b$  in Fig. 1 may be stated as a linear function of the current density  $i$  in the form

$$E = A_1 - B_1 i, \quad (15)$$

where  $A_1$  and  $B_1$  are constants equal to

$$E_s \text{ and } K \left( \frac{Q}{Q - it} \right) + L, \quad (16)$$

respectively.

A fairly good fit to Eq. (15) is shown in Fig. 2 where  $E$  has been plotted as a function of  $i$  for five values of  $it$  using the discharge data for the lead-zinc cell shown in Appendix Fig. A24. The potentials,  $E$  at the current density,  $i = 0.079\text{C amp/cm}^2$ , were considerably lower than the straight lines drawn through the corresponding values of  $it$ , thus showing that this particular discharge was out of agreement with the remainder of the data. Variations this large were not observed as a rule. The remainder four values of  $i$  gave good straight line fits in Fig. 2. Either of the two low values of  $i$  could be used for  $i_a$  and either of the two high values could be used for  $i_b$ . As a rule a plot of  $E$  vs  $i$  for each of two values of  $it$  will be sufficient to select satisfactory values of  $i_a$  and  $i_b$ . Points such as A which were taken past the knee of the discharge curve should not be used in making up these charts of  $E$  vs  $i$ . Very

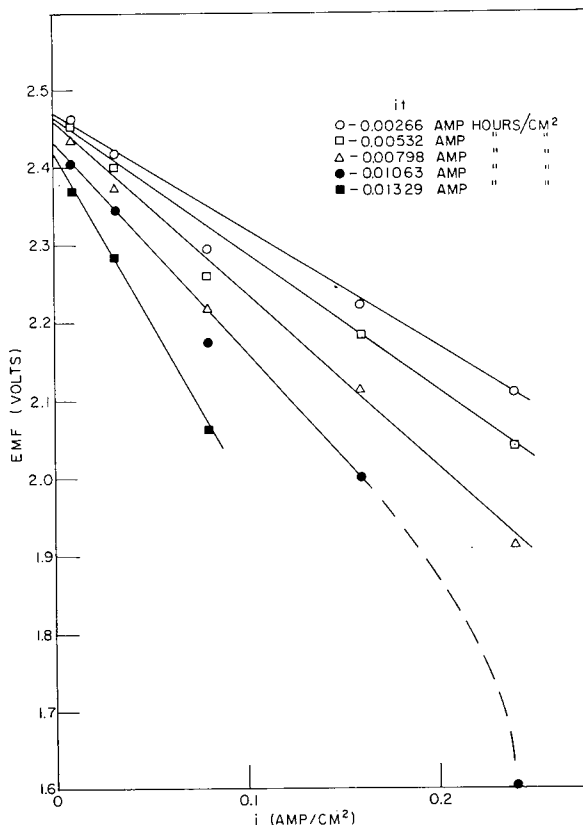


Fig. 2 - Potential during discharge as a function of current density for various values of  $it$

low values and very high values of  $i$  are avoided if feasible in selecting  $i_a$  and  $i_b$  since these extreme values have a tendency to be less accurate. With a little experience,  $i_a$  and  $i_b$  often can be selected on the basis of judgment without drawing up a chart such as that shown in Fig. 2.

If Eq. (10) is a perfect fit for the discharge data, then the plot of  $E$  vs  $i$  as illustrated in Fig. 2 would consist of straight lines intersecting on the  $E$  axis at  $E = E_s$ . If the plot of  $E$  vs  $i$  gives lines that do not intersect on the  $E$  axis or if they are curves, then Eq. (10) does not describe the discharge data perfectly. However, Eq. (10) is so adaptable that it can describe such cases with good accuracy and it has not been necessary to reject any data on this account.

Discharge data was not accepted for study here whenever it was so erratic and full of error that a plot of  $E$  vs  $i$  did not give some semblance of a smooth curve. It was found that all of the data that were acceptable on this basis could be fitted by Eq. (10). Virtually all of the room temperature discharge data taken from the literature were found to be acceptable. At low temperatures the available data was more erratic and less acceptable.

The points 1, 2, 3, and 4, used to calculate the numerical values of the parameters  $K$ ,  $Q$ , and  $L$ , are selected in the manner illustrated in Fig. 3 which duplicates the two discharge curves in Fig. 1. A tangent is drawn to the high current density discharge curve at point  $d$  and point  $f$  is selected to be 0.1 volt below the tangent line. Point  $d$  is determined by eye by laying a transparent plastic straight edge tangent to the curve and adjusting the point of tangency until  $i_b t_d$  equals  $0.5 i_b t_f$ . This method is rapid and sufficiently accurate. Point  $e$  is located in a manner similar to  $f$ .

The value of  $E$  for point 3 is approximately 0.03 volt greater than it is for point  $f$ . The value of  $E$  for point 4 is approximately 0.02 volt greater than it is for point  $e$ . Point 1 is chosen so  $i_b t_1$  equals approximately  $0.5 i_b t_3$ . If  $i_b t_f / i_a t_e$  is less than 0.7, point 2 is chosen directly above point 3 so that  $i_a t_2$  will equal  $i_b t_3$ . If  $i_b t_f / i_a t_e$  is greater than 0.7, point 2 is chosen directly above point one so that  $i_a t_2$  will equal  $i_b t_1$ . This procedure gives an approximate location of the points which supply the numerical data to

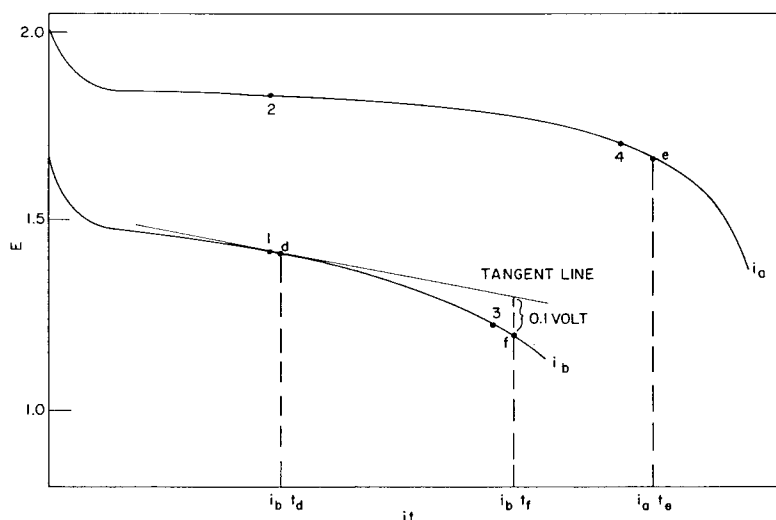


Fig. 3 - Selection of data to be used in numerical calculations

substitute in Eqs. (14) and (13), and make possible the calculation of numerical values of K, Q, L and  $E_s$  which can be substituted in Eq. (10) to give a fairly good numerical description of the discharge data. Values of E vs  $i_t$  for different discharge rates can be calculated from this equation and compared to the actual discharge data. If the agreement is not good enough, it can be improved by the method of successive approximations. A new calculation can be made using slightly different locations for one or more of the four points on the two discharge curves,  $i_a$  and  $i_b$ . If the calculated points were too far away from the measured results in the area to the left of some point such as 4, it could be corrected by selecting a new location for point 4 which would be slightly to the left of the old location and calculating a new numerical equation. The points calculated by this new equation to the right of point 4 would be a little farther away from the true data as a rough rule than those calculated from the first equation. A fairly good fit should be obtained with the first calculated equation. A very good fit will have been obtained by the third calculation and each calculation should take less than one hour of time.

Table 1  
Value of Selected Points from  
Lead Acid Cell Discharge Data

	$i_a = 20$		$i_b = 100$	
	$i_t$	E	$i_t$	E
1	45	1.841	40	1.848
2	90	1.988	95	1.984
3	90	1.713	95	1.674
4	180	1.837	200	1.725

The values of the 4 points, selected by the method illustrated in Fig. 3 using the lead acid discharge data from Appendix Fig. A5, are shown in the  $i_a$  columns of Table 1. The third and final selection of points are shown in the  $i_b$  columns of Table 1.

If the data from the  $i_b$  columns are substituted in Eq. (14)

$$\frac{1.984 - 1.725}{1.848 - 1.674} = \frac{20}{100} \left( \frac{200 - 95}{95 - 40} \right) \left( \frac{Q - 40}{Q - 200} \right),$$

then  $Q = 255.2$ .

Substituting in Eq. (13)

$$1.984 - 1.725 = 20 K \left[ \frac{255.2 (200 - 95)}{(255.2 - 200) (255.2 - 95)} \right],$$

then  $K = 0.004274$ .

From Eq. (11)

$$E_1 = 1.848 = E_s - 100 L - 0.5069.$$

Similarly

$$E_2 = 1.984 = E_s - 20 L - 0.1362.$$

Solving for  $E_s$  and L gives

$$E_s = 2.0615$$

and

$$L = -0.002934.$$

The calculations thus far are sufficient to give a numerical evaluation of Eq. (9), which is plotted in Fig. 1 as a dotted line from a to b and a solid line from b to c. The difference in potential  $\Delta E$  between this calculated dotted line of Eq. (9) and the true discharge potential is approximated by the term  $Ae^{-Bi^t/Q}$  in Eq. (10). In Table 2, values of  $\Delta E$  vs  $i_t$  are given for each discharge curve of the Edison cell shown in Appendix Fig. A1.

Table 2  
Values of  $\Delta E$  in Volts

i	$it$ (amp-hr/cell)						
	2	5	10	20	30	50	65
2	0.116	0.106	0.091	0.068	0.045	0.019	0.007
10	0.133	0.118	0.088	0.057	0.037	0.013	0.002
20	0.145	0.123	0.087	0.050	0.032	0.008	0.000
40	0.144	0.120	0.084	0.048	0.027	0.006	0.000
60	0.141	0.117	0.087	0.056	0.030	0.008	0.002
80	0.140	0.115	0.086	0.056	0.031	0.003	0.001
100	0.143	0.123	0.085	0.049	0.026	0.009	0.003
120	0.153	0.118	0.085	0.049	0.025	0.010	0.000
Ave.	0.139	0.118	0.087	0.044	0.032	0.0095	0.0018

The average values of  $\Delta E$  vs  $it$  in Table 2 are plotted on semilog paper in Fig. 4 and fitted by a straight line whose equation is  $\Delta E = Ae^{-B(it)^{1/2}/Q}$ . The intercept on the ordinate gives the numerical value of A. The numerical value of  $B/Q$  can be calculated from the slope or from a single point taken on the straight line. In nearly all cells the slope of the straight line is much steeper and consequently the value of  $\Delta E$  is much less at high values of  $it$  than in the example shown in Fig. 4 where  $\Delta E = 0.006$  volts at  $it = 50$ . If points 1 and 2 were chosen in Appendix Fig. A1 at  $it = 50$  then a correction of  $\Delta E = 0.006$  volts should be subtracted from the values of  $E_1$  and  $E_2$  to be used in calculating the constants in Eq. (10). This value of  $\Delta E$  could not be estimated accurately until after the first calculation had been made.

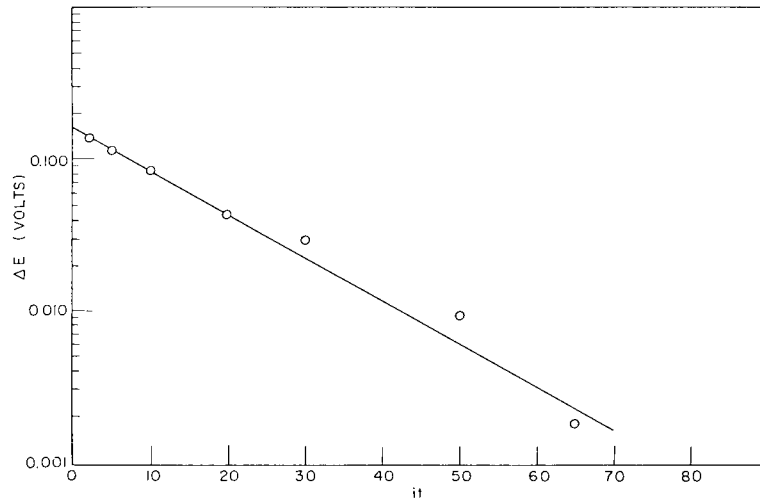


Fig. 4 - Determination of  $\Delta E$  from numerical data

#### DISCUSSION OF THE EQUATION AND ITS APPLICATION

Experimental discharge data for a number of different types of batteries has been plotted as solid lines in the Appendix. The potential  $E$  is shown for various current densities,  $i$ , as a function of  $it$  which is expressed in amp-min or amp-hr per unit area or per cell where the area is not known.

For the purposes of predicting capacities, it is advisable for the end of the discharge to be taken at a point that is a constant voltage,  $w$ , less than the voltage at point  $a$  in Fig. 1. This defines the potential at the end of the discharge as  $E_p = E_s - Ki - Li - w$ . If  $w$  is too small in value, the end-point potential will not be past the knee of the curve. If  $w$  is too large, much of the published discharge data will not extend as far as the calculated end point. A value of  $w$  equal to 0.25 volt was found to give a good compromise. Thus the potential at the end of the discharge is  $E_p = E_s - Ki - Li - 0.25$  and is calculated from Eq. (10). The discharge data in the Appendix has been shown as a solid line down to the end point  $E_p$ . Wherever the data extended below the end point, it has been shown as a dotted line.

Equation (10) has been fitted numerically to each set of discharge data thus obtaining a different numerical equation for each chart in the Appendix. The numerical values of the constants for each of these equations are shown in Appendix Table A1. The points are calculated from these equations. It can be seen that the calculated points give good fits in every case to the solid lines that represent the actual discharge data. Most of the discharge data were taken from the literature and selected to cover as wide a range of current densities as possible. All of the data fitted by Eq. (10) are shown in the Appendix and no individual discharge curves have been omitted.

Unfortunately the amount of low temperature discharge data was limited and much of it was erratic when tested by the method illustrated in Fig. 2. Heat is generated inside a battery during discharge due to its internal resistance and consequently an appreciable rise in battery temperature can occur during a high rate discharge. Thus a series of discharges made at a constant ambient temperature would show that the average battery temperature increased during discharge with increase in the current density  $i$  and in addition would be affected by a number of factors such as cell construction. The effect on the discharge curves would generally be small at room temperature where the rate of change of potential and capacity with temperature is generally small. At low temperatures, where the rate of change of potential and capacity with temperature is generally large, the high rate discharges could be changed appreciably and might make it difficult to apply Eq. (10) in some cases.

In Appendix Figs. A2, A3, and A12, the discharge took place in two steps and it was found that a separate equation could be fitted to each step. Two sets of equation coefficients are provided in Appendix Table A1 for these cases. For example, the equation for the silver cell in Appendix Fig. A2 would be

$$E = 1.8310 - 0.005138 \left( \frac{37.06}{37.06 - it} \right) i + 0.00388 i - 0.20 e^{-0.60it}$$

or

$$E = 1.5567 - 0.0004 \left( \frac{112}{112 - it} \right) i - 0.00067 i,$$

whichever is higher.

Whenever the calculated values of  $E_s$ ,  $K$ ,  $Q$ , and  $L$  are the true values and are not affected by the choice of the four points, Eq. (10) fits that particular discharge data theoretically. Whenever the calculated values of  $E_s$ ,  $K$ ,  $Q$  and  $L$  are not the true values and are affected by the choice of points 1 to 4, Eq. (10) fits that particular discharge data empirically. As a very rough rule, a closer approach to a theoretical fit is generally found in the presence of one or more of the following conditions: the discharge data covers a narrow range of current densities, the potential drop due to polarization is low, the electrolyte does not change in composition during discharge, the slope of the discharge curves before the knee is relatively small, and the ratio  $it/Q$  is fairly large and covers

a relatively narrow range of values of  $i_t$ . Equation (10) is more apt to give an empirical fit in the presence of one or more of the following conditions: the discharge data covers a wide range of current densities, the potential drop due to polarization is high, the electrolyte varies in composition during discharge, the slope of the discharge curve before the knee is relatively large, and the ratio of  $i_t/Q$  covers a relatively wide range of values of  $i_t$ .

In any case, Eq. (10) is so adaptable that wide variations in its constants, particularly  $K$  and  $L$ , enable it to be fitted with good accuracy to a very wide range of discharge data. A large increase in the numerical value of  $K$  will be accompanied by such a large decrease in the value of  $L$  that  $L$  will often be negative in value as can be seen in Table 2. Since  $L$  is the internal resistance in the original derivation and theoretically cannot be negative in value, it is obvious that Eq. (10) must be considered to be empirical in most of its curve fitting applications.

In Fig. 2 the potential is low for the points at  $i$  equals 0.0798 amp/cm<sup>2</sup>. In Appendix Fig. A24 the calculated points at this current density are appreciably higher than the measured values thus indicating the strong likelihood of an error in the measurement. In Appendix Figs. A22 and A23, both sets of data appear to contain an error in the measured potential of one of the discharge curves. When there are only three discharge curves and two of them are correct, it is not possible to tell which one of the three is in error without collecting more data. A fourth discharge made at a different current density will, if correct, determine which of the other three curves contains the error.

On the other hand, in either Figs. A22 or A23, or both, the data could be correct in which case Eq. (10) simply does not give a very good fit to the data. This condition could be verified by making more discharges at different current densities. Since Eq. (10) is empirical in much of its application, there is no reason to believe that it should have to describe fully the discharge of every type of battery.

An examination of the Appendix shows that the difference between the results calculated from Eq. (10) and the measured results are often larger at the highest current densities than they are at intermediate current densities. This larger variation can be attributed to the high relative dispersion of the data; the fact that the highly simplified calculation methods given here tend to give the poorest fit at high current densities; and the fact that the poorest fit is often obtained at the extreme limits when fitting equations to measured data.

A study of the Appendix shows a tendency for a few of the calculated curves at the lowest current density to have less slope and a smaller capacity than the observed data. This condition is most noticeable in Figs. A24 and A25 and seems to be most generally associated with batteries whose electrolytes change appreciably in concentration during discharge.

As a rough empirical approximation, it is assumed that the drop in potential in a battery is directly proportional to the change in electrolyte concentration during discharge, assuming all other factors are neglected. Equation (10) can then be written as

$$E = E_s - K \left( \frac{Q}{Q - i t} \right) i - Li + Ae^{-B i t / Q} - C i t, \quad (17)$$

where  $C$  is a constant.

To determine the numerical value of  $C$  select four points as shown in Fig. 5 which are far enough past the initial potential drop for the exponential term to be negligible.

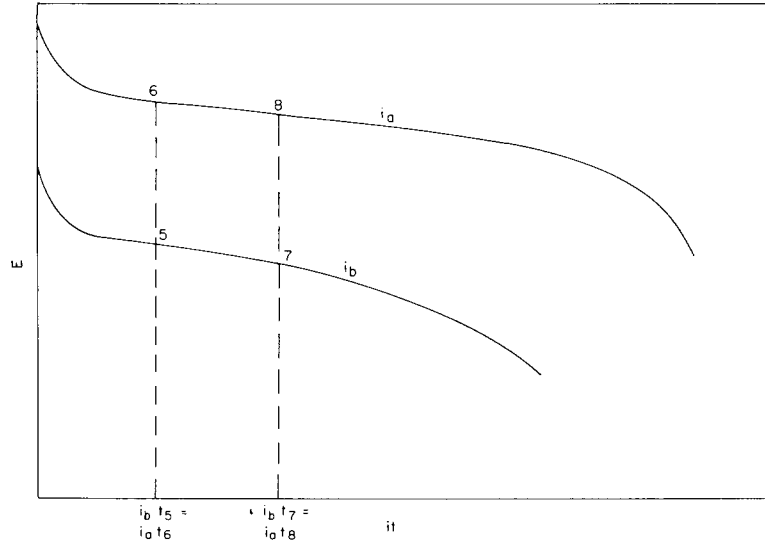


Fig. 5 - Typical discharge curves to be used in numerical calculation of C

From Eq. (17)

$$E_5 = E_s - K i_b \left( \frac{Q}{Q - i_b t_5} \right) - L i_b - C i_b t_5 \tag{18}$$

$$E_7 = E_s - K i_b \left( \frac{Q}{Q - i_b t_7} \right) - L i_b - C i_b t_7 \tag{19}$$

Subtracting Eq. (19) from Eq. (18) gives

$$E_5 - E_7 = K i_b \left[ \frac{Q}{Q - i_b t_7} - \frac{Q}{Q - i_b t_5} \right] + C (i_b t_7 - i_b t_5) \tag{20}$$

Similarly

$$E_6 - E_8 = K i_a \left[ \frac{Q}{Q - i_b t_7} - \frac{Q}{Q - i_b t_5} \right] + C (i_b t_7 - i_b t_5) \tag{21}$$

From Eq. (20) and Eq. (21)

$$C = \frac{i_b (E_6 - E_8) - i_a (E_5 - E_7)}{(i_b - i_a)(i_b t_7 - i_b t_5)} \tag{22}$$

Numerical values of C are calculated from Eq. (22) and substituted in Eq. (17).

Let  $E' = E + C it$ .

Then  $E'_1 = E_1 + C i_b t_1$ ,  $E'_2 = E_2 + C i_a t_2$ ,  $E'_3 = E_3 + C i_b t_3$ , and  $E'_4 = E_4 + C i_a t_4$ . If  $E'_1$ ,  $E'_2$ ,  $E'_3$  and  $E'_4$  are substituted for  $E_1$ ,  $E_2$ ,  $E_3$ , and  $E_4$ , respectively, in Eqs. (11) to (15), they can be used to calculate numerical values of Q, K, L, and  $E_s$  in the manner previously described.

Numerical values of Eq. (17) were determined in this manner for the lead-zinc cell and the fluoboric acid cell shown in Appendix Figs. A24 and A25 and found to be

$$E = 2.4775 - 0.9237 \left( \frac{0.0181}{0.0181 - it} \right) i - 0.4295 i - 4.25 it ,$$

$$E = 1.7104 - 0.00142 \left( \frac{23.445}{23.445 - it} \right) i - 0.00013 i - 0.006 it ,$$

respectively.

Calculated points from these equations are shown in Figs. 6 and 7 to give very good fits to the experimental data.

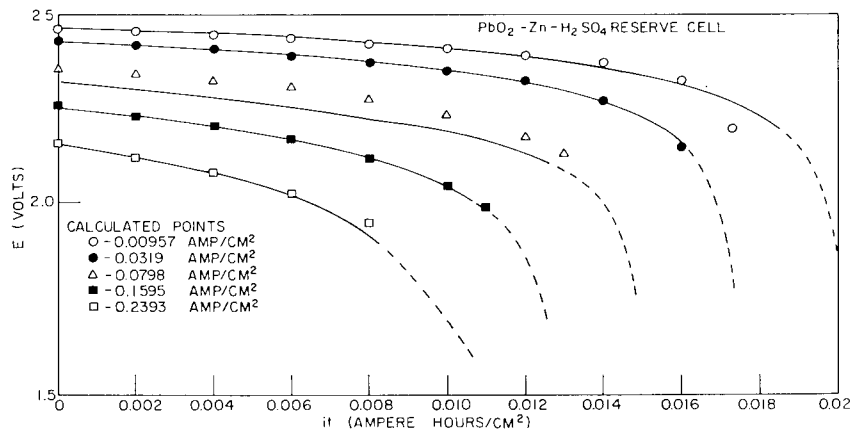


Fig. 6 - Example of improved fit of discharge data by use of Eq. (17)

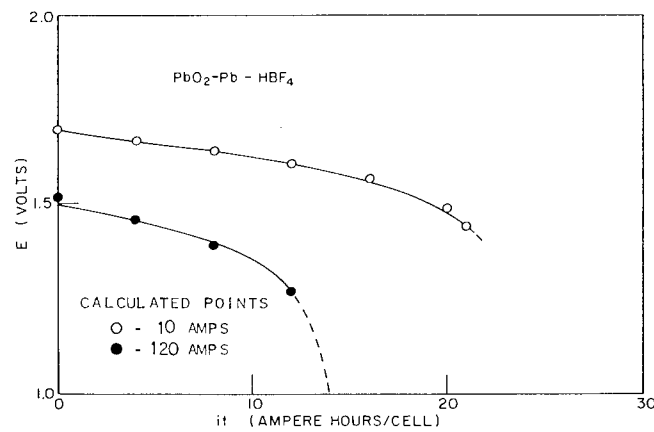


Fig. 7 - Example of improved fit of discharge data by use of Eq. (17)

## CONCLUSIONS

It has been shown for a large number of batteries that the potential of a battery during discharge over a wide range of current densities can be described very adequately by the equation

$$E = E_s - K \left( \frac{Q}{Q - it} \right) i - Li + Ae^{-Bt/Q},$$

where  $E_s$ ,  $K$ ,  $Q$ ,  $L$ ,  $A$ , and  $B$  are constants,  $i$  is the current density and  $t$  is time, and  $K$ ,  $Q$ , and  $L$  correspond to the coefficient of polarization, the available quantity of electricity, and the internal resistance, respectively. In the derivation of Eq. (10) it was assumed that the potential drop due to polarization was a linear function of a current density which was proportional to the amount of current flowing per unit weight of unused active material at a given time. The fact that this assumption was effective shows the adaptability of Eq. (10) but does not prove that the assumption is true for the wide range of conditions in which Eq. (10) can be successfully applied. In its practical applications, the numerical values of  $K$ ,  $Q$ , and  $L$  that were derived from the experimental discharge data often did not correspond to the true values and consequently had no physical significance. To that extent Eq. (10) must be considered to be an empirical equation.

A simple method is described for calculating the numerical values of the equation constants from the experimental discharge data. The equation gives an excellent description of a large variety of battery discharges and can be used to advantage in interpolating and extrapolating. It makes possible a complete description of battery discharge characteristics, using a minimum of experimental data and at the same time pinpointing experimental errors in the discharge data.

Appendix

ACTUAL DISCHARGE DATA USED FOR CALCULATION  
OF THE BATTERY DISCHARGE EQUATION

These graphs are discharge data which were used by the author to test the battery discharge equation (Eq. 10). In these charts the solid lines represent actual discharge data. The points were calculated from Eq. (10) using the methods described in this report.

Table A1  
Equation Coefficients

Fig.	$E_s$	K	Q	L	A	B/Q	Temp (°C)	Ref.
A1	1.308	0.0003936	115.403	0.00390	0.165	0.06564	Room Temp	A1
A2 (1)	1.831	0.005138	37.06	-0.00388	0.020	0.60	27	A2
A2 (2)	1.5567	0.00040	112.0	0.00067	-	-	27	A2
A3 (1)	1.3733	0.00831	28.68	-0.00543	-	-	27	A3
A3 (2)	1.0990	0.0026	95.753	-0.000965	-	-	27	A3
A4	1.2112	3.464	4.171	-2.579	0.090	7.525	21	A4
A5	2.0615	0.004274	255.2	-0.002934	-	-	Room Temp	A5
A6	1.3150	0.00718	5.623	0.07907	0.18	1.72	Room Temp	A6
A7	1.1846	0.0683	58.68	-0.02045	0.060	0.3465	21	A7
A8	2.1180	0.006888	3.07	0.00264	-	-	27	A8
A9	1.0940	0.1059	0.891	0.44	-	-	20	A9
A10	1.3032	0.03806	742.7	0.1684	0.060	0.044	21	A10
A11	1.5761	0.1287	0.8608	0.2114	-0.214	48.43	Room Temp	A3
A12 (1)	1.3153	0.0284	2.171	0.00375	-	-	Room Temp	A3
A12 (2)	1.0640	0.00526	8.162	0.00218	-	-	Room Temp	A3
A13	1.3273	0.0948	810.4	0.1469	0.040	0.0222	21	A11
A14	1.2743	0.3343	25.61	-0.269	0.360	2.197	25	A3
A15	2.003	0.01894	58.31	-0.0150	-	-	25	A12
A16	1.2500	0.0250	0.953	0.0060	0.095	3.83	27	A13
A17	1.7477	0.0236	46.72	-0.00159	-	-	25	A14
A18	0.6750	0.004673	588.06	0.02713	0.050	0.00805	21	A11
A19	1.6785	0.0354	6.846	-0.0215	0.106	1.528	20	A15
A20	1.2021	0.001358	74.67	-0.000241	0.080	0.1386	-18	A16
A21	1.1902	0.0367	91.37	-0.03176	0.090	4.394	-54	A16
A22	2.1440	0.233	0.0142	3.130	-	-	27	A17
A23	1.6861	0.0638	0.7492	0.0018	-0.026	26.24	0	A18
A24	2.4607	0.9722	0.01737	0.3589	-	-	27	A19
A25	1.6383	0.0016	22.135	-0.000459	-	-	27	A20

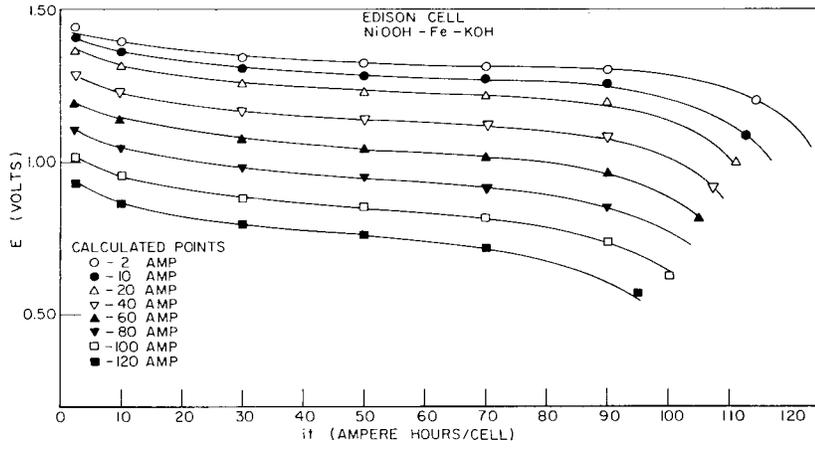


Figure A1

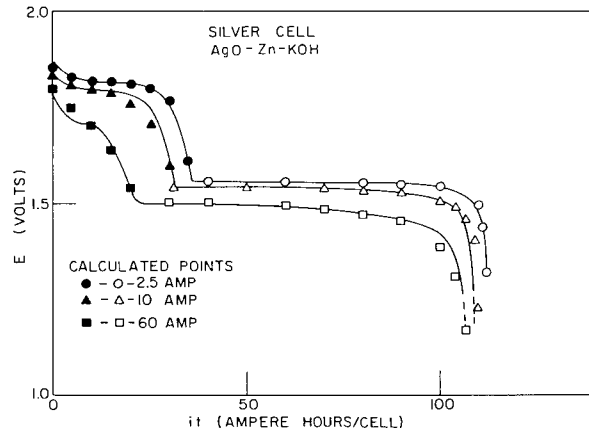


Figure A2

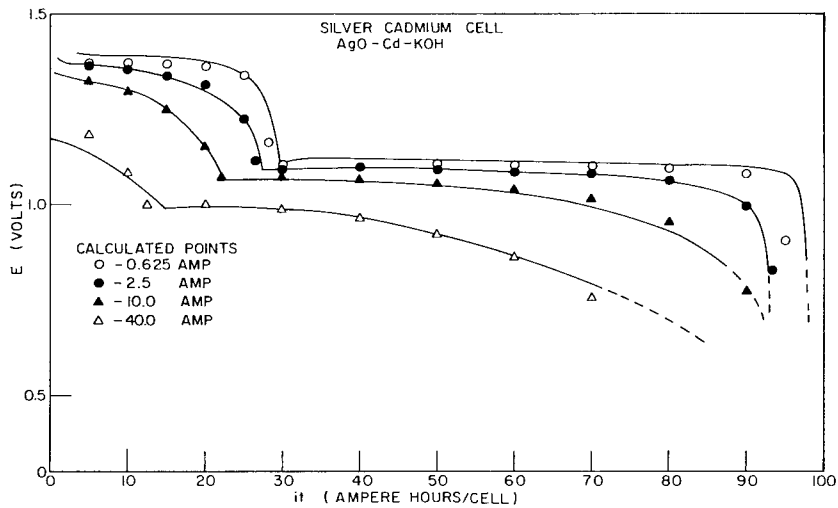


Figure A3

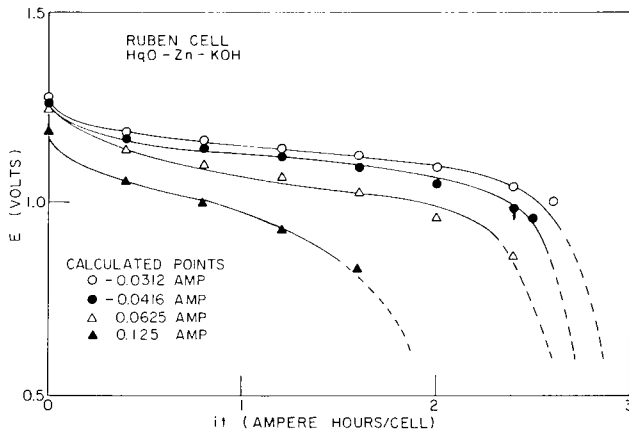


Figure A4

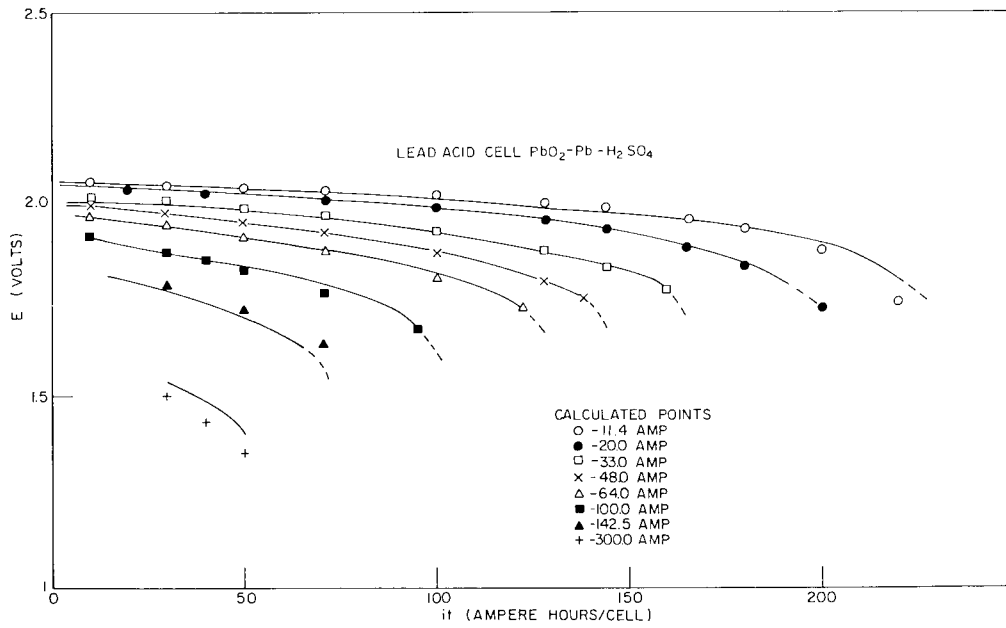


Figure A5

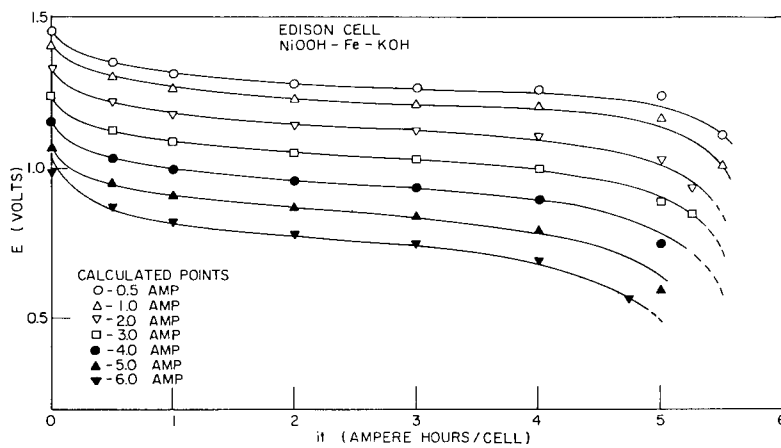


Figure A6

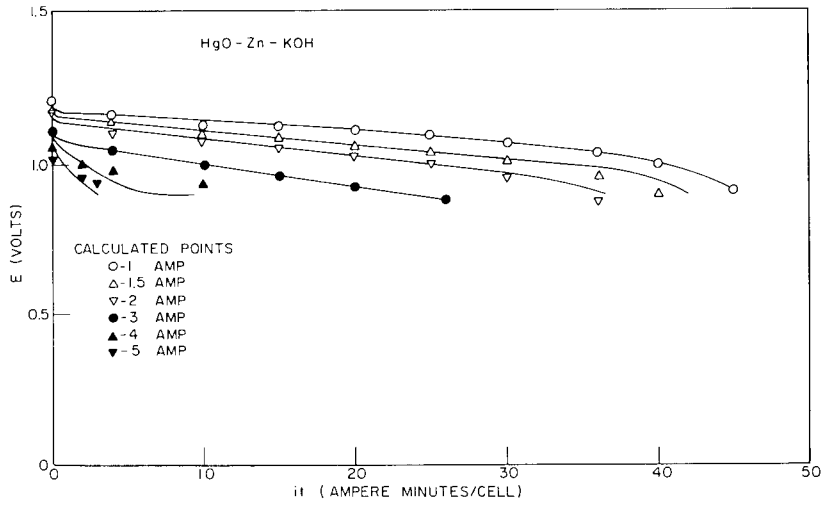


Figure A7

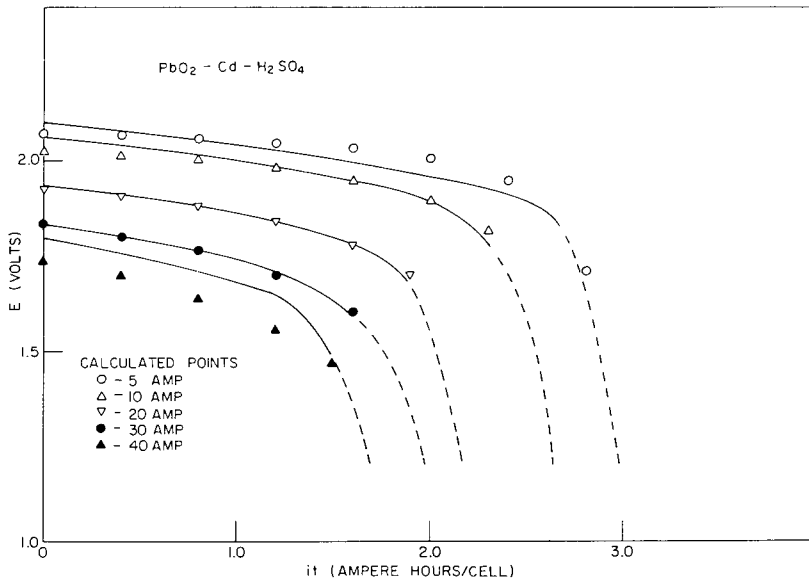


Figure A8

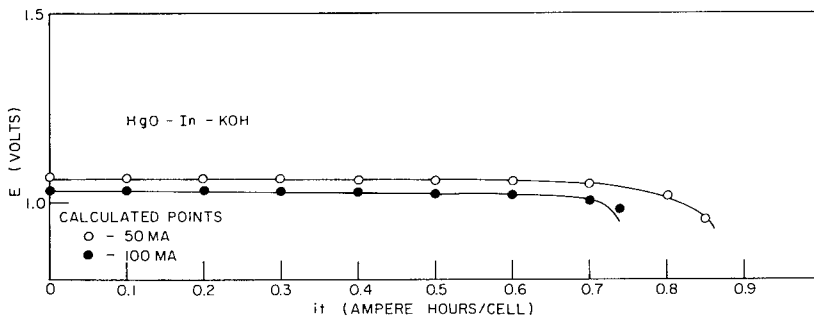


Figure A9

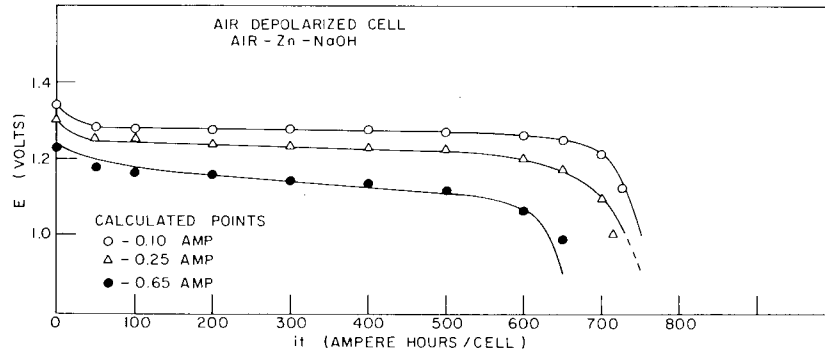


Figure A10

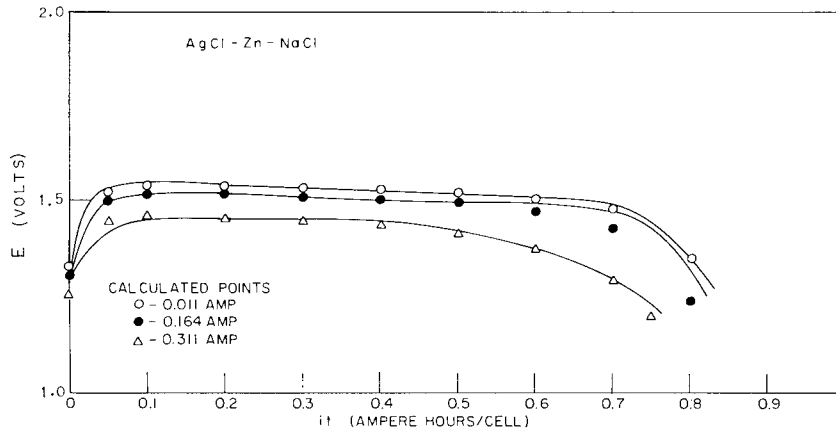


Figure A11

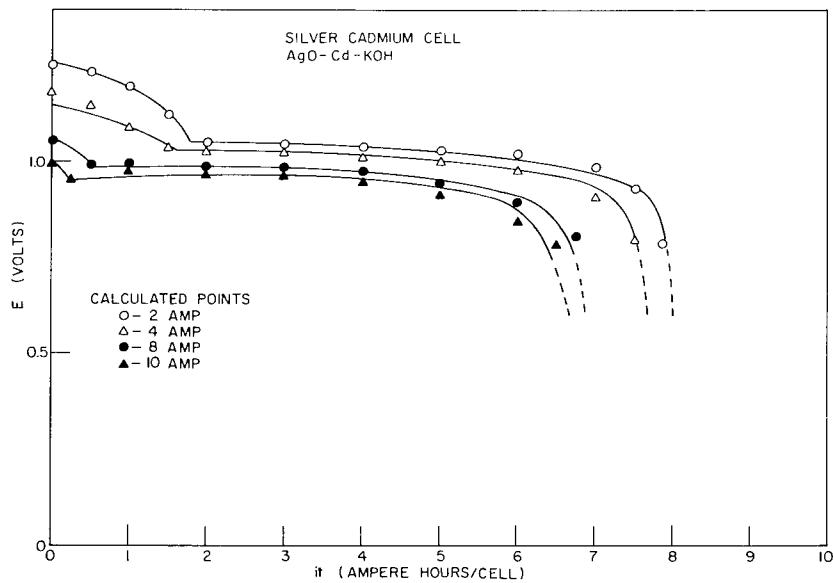


Figure A12

Figure A13

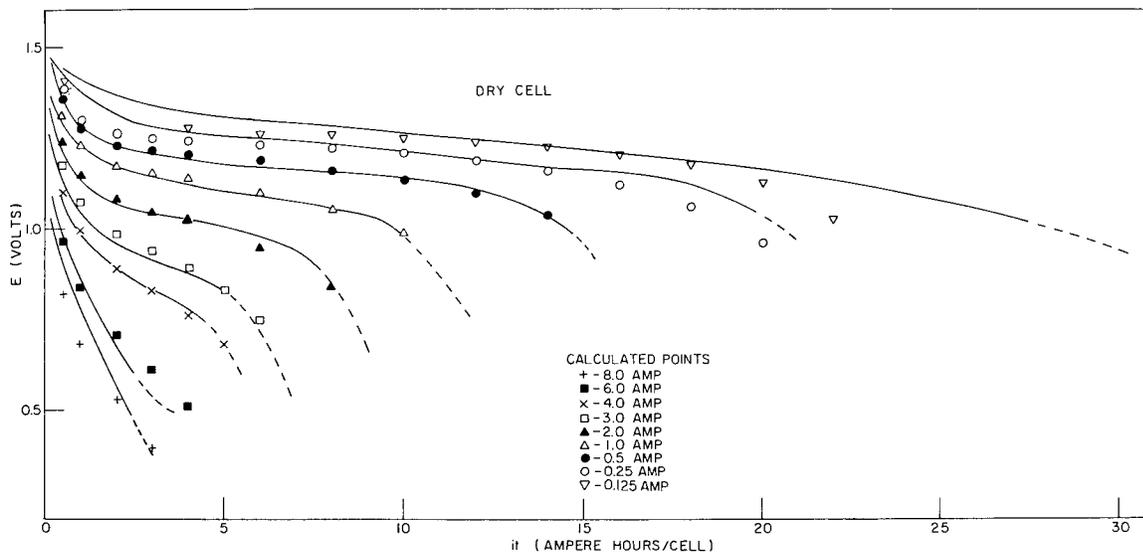
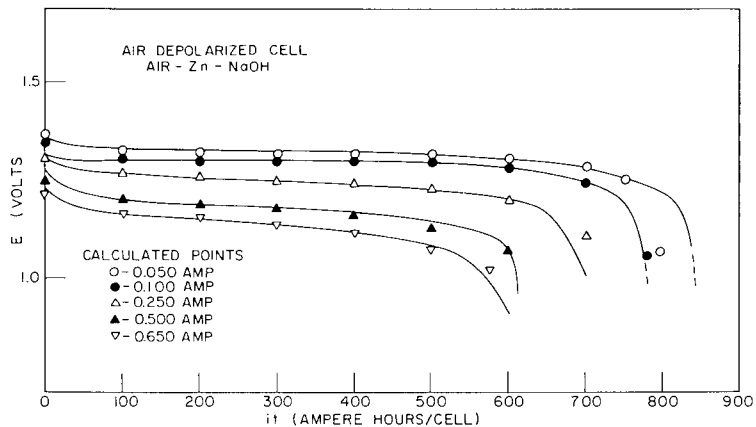


Figure A14

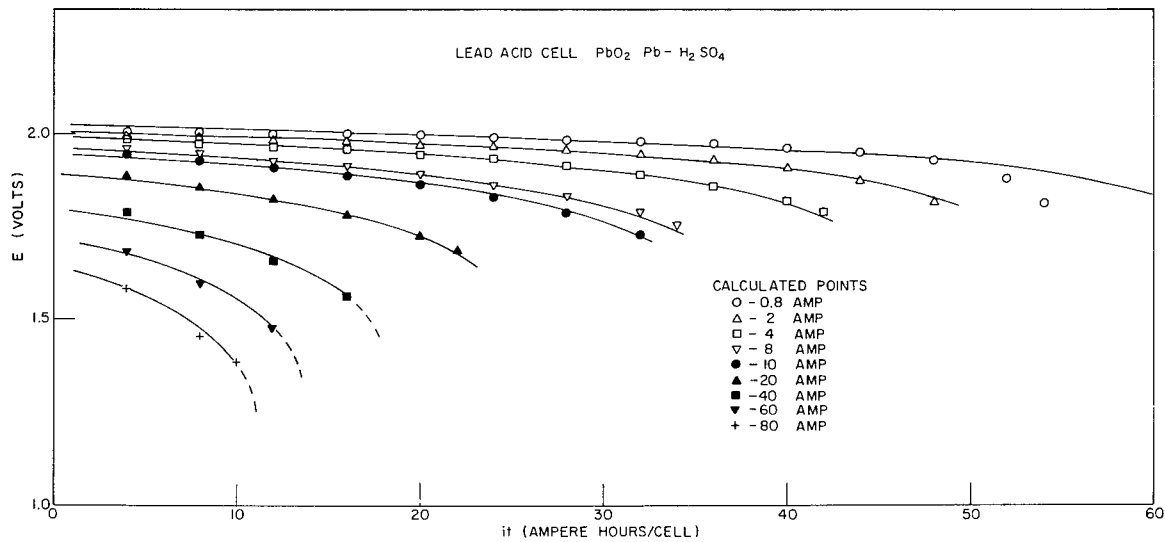


Figure A15

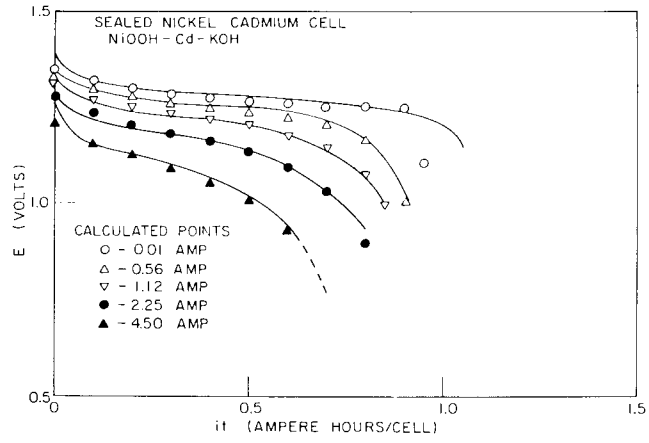


Figure A16

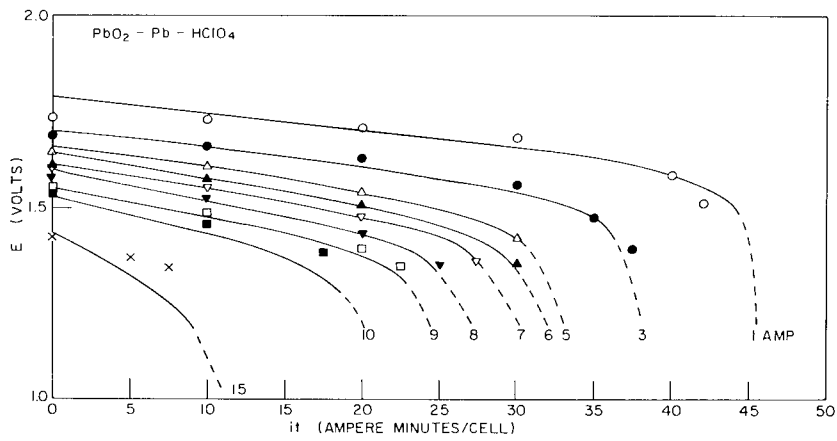


Figure A17

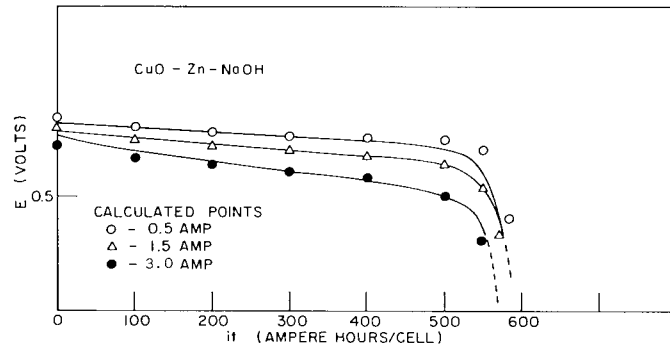


Figure A18

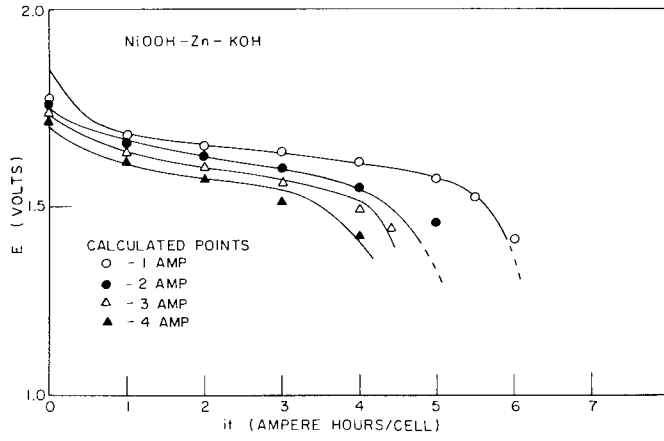


Figure A19

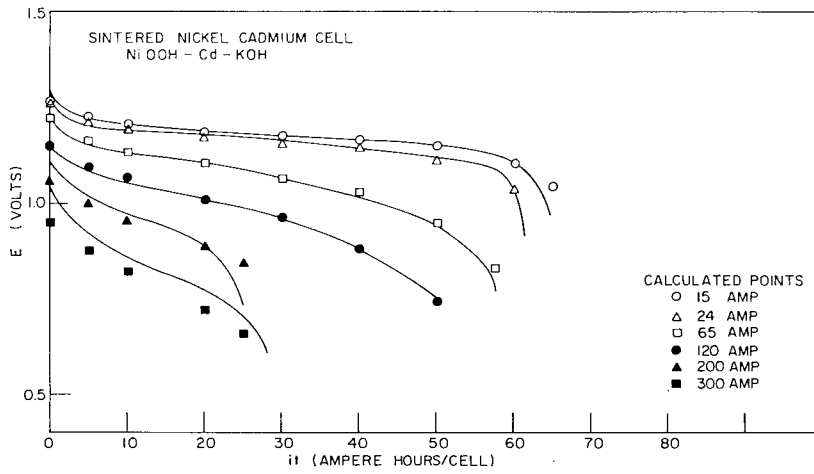


Figure A20

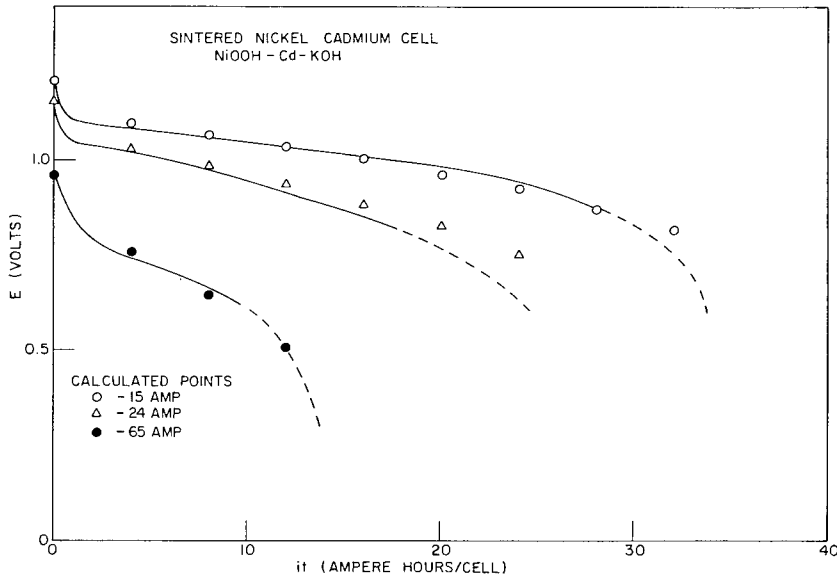


Figure A21

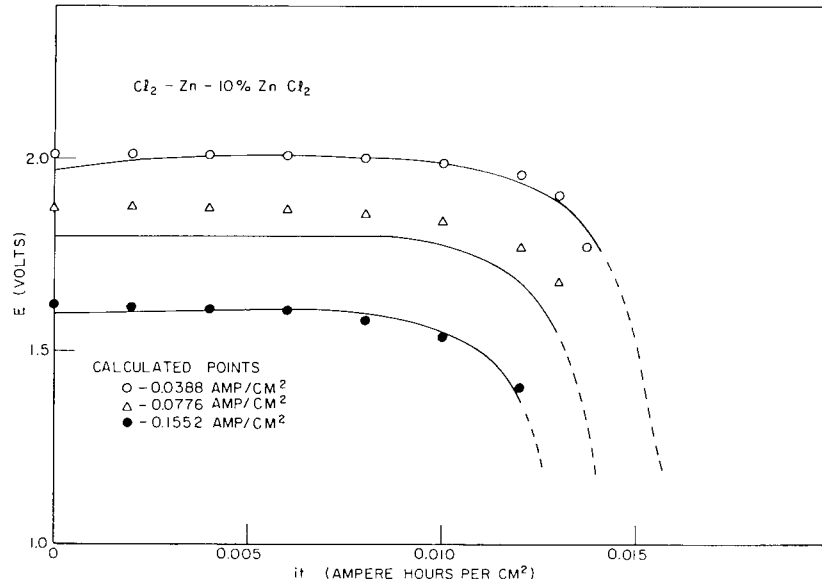


Figure A22

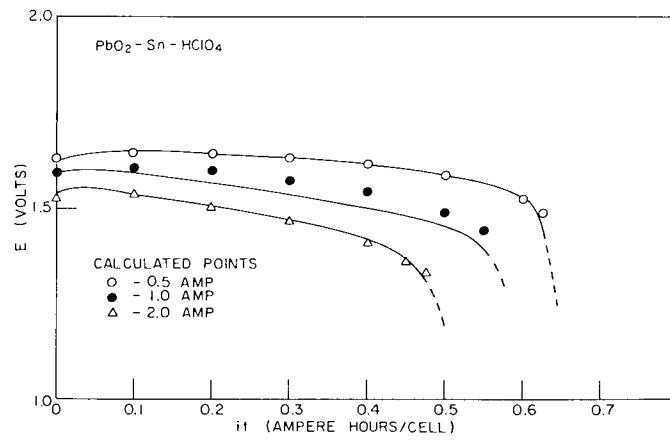


Figure A23

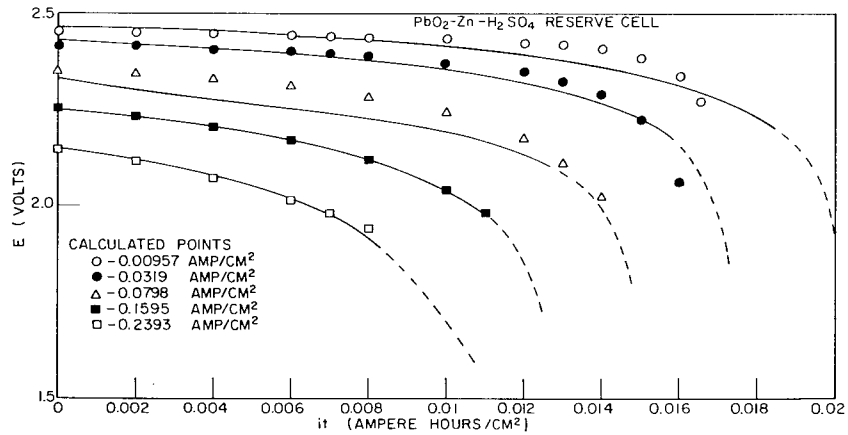


Figure A24

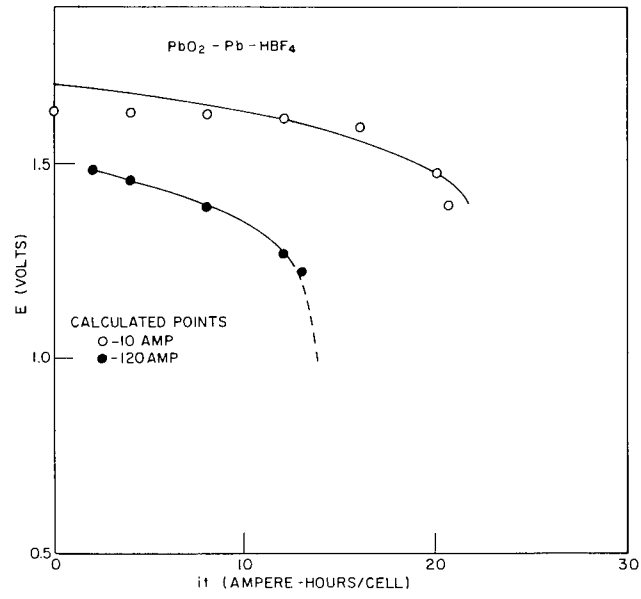


Figure A25

REF ID: A70700

## REFERENCES

- A1. Anderson, F. C., *J. Electrochem. Soc.* 99:244C (1952)
- A2. Wales, C. P., "Silver Oxide-Zinc Alkaline Storage Batteries: Effect of Float and Normal Charges on Capacity and Related Characteristics," *NRL Report 5167*, Aug. 1958
- A3. Wales, C. P., unpublished data
- A4. Friedman, M., and McCauley, C., *Trans. Electrochem. Soc.* 92, 195 (1947)
- A5. "Akkumulatoren - Handbuch der AFA," *Accumulatoren-Fabrik Aktiengesellschaft*, p. 112
- A6. Vinal, G. W., "Storage Batteries," 4th ed., New York:John Wiley and Sons, Inc., p. 230, p. 267, 1955
- A7. Daniel, A. F., "The Zinc-Mercuric Oxide System," *Symposium on Batteries*, 22-23 April 1952. Sponsored by the Committee on Equipment and Supplies on Guided Missiles, Research and Development Board, Washington, D.C.
- A8. Pucher, L. E., *J. Electrochem. Soc.* 99, 204C (1952)
- A9. Lewis, R. W., and Partridge, A. H., "Proceedings of the Second International Symposium on Batteries," *Christchurch, Hants, England, Signals Research and Development Establishment, Paper 2/1*
- A10. Vinal, G. W., "Primary Batteries," New York:John Wiley and Sons, Inc., p. 222 (1950)
- A11. Schumacher, E. A., and Heise, G. W., *J. Electrochem. Soc.* 99, 191C (1952)
- A12. Hoxie, E. A., *Transactions of the American Institute of Electrical Engineers, Part II Applications and Industry*, 73, 17 (1954)
- A13. Wales, C. P., "Sealed Nickel-Cadmium Cells," *NRL Memorandum Report 967*, Aug. 1959
- A14. Pierce, R. T., Baldwin, J. H., McMurtrie, R. L., and Power, W. H., "Characteristics of the Perchloric Acid Battery," *NRL Report P-2307*, June 1944
- A15. Romanov, V. V., Lukovtsev, P. D., Kharchenko, G. N., and Sandler, P. I., *Zhurnal Prikladnoi Khimii* 33, 1556 (1960)
- A16. Ellis, G. B., Mandel, H., and Linden, D., *J. Electrochem. Soc.* 99, 250C (1952)
- A17. Howard, P. L., *J. Electrochem. Soc.* 99, 206C (1952)
- A18. Brook, P. A., and Davies, A. E., *J. Appl. Chem.* 6, 174 (1956)

- A19. Schlotter, W. J., J. Electrochem. Soc. 99, 205C (1952)
- A20. Schrodt, J. P., and Craig, D. N., "Lead Perchloric and Fluoboric Acid Battery," Symposium on Batteries, 22-23 April 1952, Sponsored by the Committees on Equipment and Supplies on Guided Missiles, Research and Development Board, Washington, D.C.

DOCUMENT CONTROL DATA - R&D		
<i>(Security classification of title, body of abstract and indexing annotation must be entered when the overall report is classified)</i>		
1. ORIGINATING ACTIVITY <i>(Corporate author)</i> U.S. Naval Research Laboratory Washington, D.C. - 20390		2a. REPORT SECURITY CLASSIFICATION Unclassified
		2b. GROUP --
3. REPORT TITLE "Theoretical Design of Primary and Secondary Cells. Part IV - Further Studies of the Battery Discharge Equation"		
4. DESCRIPTIVE NOTES <i>(Type of report and inclusive dates)</i> Interim		
5. AUTHOR(S) <i>(Last name, first name, initial)</i> Shepherd, C.M.		
6. REPORT DATE November 16, 1964	7a. TOTAL NO. OF PAGES 29	7b. NO. OF REFS 20
8a. CONTRACT OR GRANT NO. CO5-14	9a. ORIGINATOR'S REPORT NUMBER(S) NRL Report 6129	
b. PROJECT NO. SF 013-06-03-4366		
c. and RR 001-01-43-4755	9b. OTHER REPORT NO(S) <i>(Any other numbers that may be assigned this report)</i>	
d.		
10. AVAILABILITY/LIMITATION NOTICES Unlimited Distribution		
11. SUPPLEMENTARY NOTES	12. SPONSORING MILITARY ACTIVITY	
13. ABSTRACT <p>An equation has been derived describing a complete battery discharge for the case where the current density is constant. The battery potential during discharge is given as a function of time, current density, polarization, internal resistance, and other factors. This equation has a number of practical applications. It can be used to describe battery charges, discharges, capacities, power evolution, and to predict capacities and locate errors in experimental data. A simplified numerical system has been developed for determining the equation constants from the experimental data.</p>		

14. KEY WORDS	LINK A		LINK B		LINK C	
	ROLE	WT	ROLE	WT	ROLE	WT
Battery Discharge Equation						
Current density						
Battery capacities						
Internal resistance						
Polarization						
Battery charges						
Battery discharges						
Primary cells						
Secondary cells						
Theoretical design						
Cell potential						
Discharge time						
Cells						
Batteries						

INSTRUCTIONS

1. **ORIGINATING ACTIVITY:** Enter the name and address of the contractor, subcontractor, grantee, Department of Defense activity or other organization (*corporate author*) issuing the report.

2a. **REPORT SECURITY CLASSIFICATION:** Enter the overall security classification of the report. Indicate whether "Restricted Data" is included. Marking is to be in accordance with appropriate security regulations.

2b. **GROUP:** Automatic downgrading is specified in DoD Directive 5200.10 and Armed Forces Industrial Manual. Enter the group number. Also, when applicable, show that optional markings have been used for Group 3 and Group 4 as authorized.

3. **REPORT TITLE:** Enter the complete report title in all capital letters. Titles in all cases should be unclassified. If a meaningful title cannot be selected without classification, show title classification in all capitals in parenthesis immediately following the title.

4. **DESCRIPTIVE NOTES:** If appropriate, enter the type of report, e.g., interim, progress, summary, annual, or final. Give the inclusive dates when a specific reporting period is covered.

5. **AUTHOR(S):** Enter the name(s) of author(s) as shown on or in the report. Enter last name, first name, middle initial. If military, show rank and branch of service. The name of the principal author is an absolute minimum requirement.

6. **REPORT DATE:** Enter the date of the report as day, month, year, or month, year. If more than one date appears on the report, use date of publication.

7a. **TOTAL NUMBER OF PAGES:** The total page count should follow normal pagination procedures, i.e., enter the number of pages containing information.

7b. **NUMBER OF REFERENCES:** Enter the total number of references cited in the report.

8a. **CONTRACT OR GRANT NUMBER:** If appropriate, enter the applicable number of the contract or grant under which the report was written.

8b, 8c, & 8d. **PROJECT NUMBER:** Enter the appropriate military department identification, such as project number, subproject number, system numbers, task number, etc.

9a. **ORIGINATOR'S REPORT NUMBER(S):** Enter the official report number by which the document will be identified and controlled by the originating activity. This number must be unique to this report.

9b. **OTHER REPORT NUMBER(S):** If the report has been assigned any other report numbers (*either by the originator or by the sponsor*), also enter this number(s).

10. **AVAILABILITY/LIMITATION NOTICES:** Enter any limitations on further dissemination of the report, other than those

imposed by security classification, using standard statements such as:

- (1) "Qualified requesters may obtain copies of this report from DDC."
- (2) "Foreign announcement and dissemination of this report by DDC is not authorized."
- (3) "U. S. Government agencies may obtain copies of this report directly from DDC. Other qualified DDC users shall request through \_\_\_\_\_."
- (4) "U. S. military agencies may obtain copies of this report directly from DDC. Other qualified users shall request through \_\_\_\_\_."
- (5) "All distribution of this report is controlled. Qualified DDC users shall request through \_\_\_\_\_."

If the report has been furnished to the Office of Technical Services, Department of Commerce, for sale to the public, indicate this fact and enter the price, if known.

11. **SUPPLEMENTARY NOTES:** Use for additional explanatory notes.
12. **SPONSORING MILITARY ACTIVITY:** Enter the name of the departmental project office or laboratory sponsoring (*paying for*) the research and development. Include address.
13. **ABSTRACT:** Enter an abstract giving a brief and factual summary of the document indicative of the report, even though it may also appear elsewhere in the body of the technical report. If additional space is required, a continuation sheet shall be attached.

It is highly desirable that the abstract of classified reports be unclassified. Each paragraph of the abstract shall end with an indication of the military security classification of the information in the paragraph, represented as (TS), (S), (C), or (U).

There is no limitation on the length of the abstract. However, the suggested length is from 150 to 225 words.

14. **KEY WORDS:** Key words are technically meaningful terms or short phrases that characterize a report and may be used as index entries for cataloging the report. Key words must be selected so that no security classification is required. Identifiers, such as equipment model designation, trade name, military project code name, geographic location, may be used as key words but will be followed by an indication of technical context. The assignment of links, roles, and weights is optional.

REF ID: A66521